Dendritic growth and synaptic organization from activity-independent cues and local activity-dependent plasticity

Jan H. Kirchner[1,2†*], **Lucas Euler**[2†], **Julijana Gjorgjieva**[1,2*]

***For correspondence:**
kirchner.jan@icloud.com;
gjorgjieva@tum.de

[†]These authors contributed equally to this work

[1]School of Life Sciences, Technical University of Munich, Freising, Germany;
[2]Computation in Neural Circuits Group, Max Planck Institute for Brain Research, Germany

Abstract Dendritic branching and synaptic organization shape single neuron and network computations. How they emerge simultaneously during brain development as neurons become integrated into functional networks is still not mechanistically understood. Here, we propose a mechanistic model in which dendrite growth and the organization of synapses arise from the interaction of activity-independent cues from potential synaptic partners and local activity-dependent synaptic plasticity. Consistent with experiments, three phases of dendritic growth – overshoot, pruning, and stabilization – emerge naturally in the model. The model generates stellate-like dendritic morphologies capturing several morphological features of biological neurons under normal and perturbed learning rules, reflecting biological variability. Model-generated dendrites have approximately optimal wiring length consistent with experimental measurements. Besides setting up dendritic morphologies, activity-dependent plasticity rules organize synapses into spatial clusters according to the correlated activity they experience. We demonstrate that a trade-off between activity-dependent and -independent factors influences dendritic growth and synaptic location throughout development, suggesting that early developmental variability can affect mature morphology and synaptic function. Therefore, a single mechanistic model can capture dendritic growth and account for the synaptic organization of correlated inputs during development. Our work suggests concrete mechanistic components underlying the emergence of dendritic morphologies and synaptic formation and removal in function and dysfunction, and provides experimentally testable predictions for the role of individual components.

Introduction

The dendrites of a neuron are intricately branched structures that receive electrochemical stimulation from other neurons. The morphology of dendrites determines the location of synaptic contacts with other neurons and thereby constrains single-neuron computations. During devel-

opment, the dendrites of many neurons grow simultaneously and become integrated into neural circuits. Dendrite development is highly dynamic; iterated addition and retraction of branches allow these dendrites to probe various potential synaptic partners before stabilizing (***Cline, 2016***; ***Richards et al., 2020***). Many intrinsic and extrinsic factors underlie the dynamics of dendritic development. In any given neuron, intrinsic expression of specific genes controls many morphological aspects, including the orientation of the dendrite in the cortex, the general abundance of dendritic branching, and the timing of growth onset (***Puram and Bonni, 2013***). Extrinsic signaling, in contrast, exerts precise control over the detailed dynamics of dendrite development via various mechanisms, including activity-dependent cell-to-cell interactions and molecular signaling (***Polleux et al., 2016***).

While many signaling molecules affect dendrite development, the brain-derived neurotrophic factor (BDNF) and its immature predecessor proBDNF are particularly crucial in the central nervous system (***Lu et al., 2005***). While exposure to BDNF leads to larger dendrites with a higher density of synapses (***McAllister et al., 1995***; ***Tyler and Pozzo-Miller, 2001***), exposure to proBDNF leads to smaller dendrites with fewer synapses (***Koshimizu et al., 2009***; ***Yang et al., 2014***). Furthermore, the precise balance of BDNF and proBDNF is essential for the organization of synapses into clusters during development (***Kirchner and Gjorgjieva, 2021***; ***Winnubst et al., 2015***; ***Kleindienst et al., 2011***; ***Niculescu et al., 2018***). Interestingly, synaptic activity triggers the cleaving of proBDNF into BDNF (***Je et al., 2012***), providing a mechanistic link between the molecular factors driving dendrite maturation and neural activity.

Activity-dependent factors are equally important in driving dendritic growth. As the sensory periphery is immature during early postnatal development, when many dendrites grow (***Leighton and Lohmann, 2016***), many developing circuits generate their own spontaneous activity. The rich spatiotemporal structure of spontaneous activity instructs the formation, removal, and change in the strength of synaptic inputs (***Sretavan et al., 1988***; ***Sakai, 2020***) and triggers the stabilization or retraction of entire dendritic branches (***Riccomagno and Kolodkin, 2015***; ***Lohmann et al., 2002***). While blocking spontaneous activity does not result in grossly different dendrite morphology, the density and specificity of synaptic connections are strongly perturbed (***Campbell et al., 1997***; ***Ultanir et al., 2007***), highlighting the instructive effect of spontaneous activity on dendritic development (***Crair, 1999***).

One influential hypothesis tying together the extrinsic signaling factors underlying dendritic development is the synaptotrophic hypothesis (***Vaughn, 1989***). According to this hypothesis, a growing dendrite preferentially extends into regions where it is likely to find synaptic partners. Once a dendrite finds such a partner, a synaptic contact forms, anchors the developing dendrite, and serves as an outpost for further dendritic growth. Conversely, loss of synaptic input to the dendrite can lead to retraction unless the remaining synapses stabilize the branch (***Lohmann et al., 2002***; ***Niell et al., 2004***; ***Haas et al., 2006***; ***Cline and Haas, 2008***; ***Riccomagno and Kolodkin, 2015***; ***Cline, 2016***). However, elaborate dendrites with morphologically defined synapses can also emerge without any synaptic transmission (***Verhage et al., 2000***; ***Cijsouw et al., 2014***), suggesting that synaptic activity influences dendritic growth but is not the only driving force. Despite the significant interest in the synaptotrophic hypothesis, we still lack a mechanistic understanding of how activity-

dependent and -independent factors combine to shape development.

To investigate interactions between known signaling factors and to synthesize information from different experimental results, computational models of dendrite development provide a fruitful direction to explore how different mechanisms can generate realistic dendritic morphologies (***Cuntz, 2016***). Previous approaches include modeling dendritic development with random branching (***Kliemann, 1987***) or as a reaction-diffusion system (***Luczak, 2006***), implementing activity-independent growth cones that sense molecular gradients (***van Veen and van Pelt, 1992***; ***Torben-Nielsen and De Schutter, 2014***), or constructing dendrites as the solution to an optimal wiring problem (***Cuntz et al., 2010***). While these approaches can generate dendrites that accurately match the statistics of developing and mature biological dendrites (***Koene et al., 2009***; ***Cuntz, 2016***), they provide limited insight into how dendritic growth interacts with synapse formation and local activity-dependent organization of synaptic inputs, hence obscuring the link between morphological variability and electrophysiological (***Gouwens et al., 2020***; ***Scala et al., 2021***) or functional (***Poirazi and Mel, 2001***; ***Poirazi et al., 2003***; ***Park et al., 2019***; ***Poirazi and Papoutsi, 2020***) synaptic and dendritic properties.

Here, we propose a mechanistic computational model for cortical dendritic development for dendrite growth and synapse formation, stabilization and elimination based on reciprocal interactions between activity-independent growth signals and spontaneous activity. Starting from neuronal somata distributed in a flat sheet of cortex, spatially distributed potential synapses drive the growth of stellate-like dendrites through elongation and branching by activity-independent cues. Upon contact, synaptic connections form and stabilize or disappear according to a local activity-dependent learning rule inspired by neurotrophin interactions based on correlated patterns of spontaneous activity (***Kirchner and Gjorgjieva, 2021***). Consistent with the synaptotrophic hypothesis, the stability of a dendritic branch depends on the stability of its synaptic contacts, with the branch likely retracting after substantial synaptic pruning. The resulting dynamic system naturally leads to the emergence of three distinct phases of dendrite development: 1) an initial overshoot phase characterized by dendrite growth and synapse formation, 2) a pruning phase during which the learning rule prunes poorly synchronized synapses, and 3) a stabilization phase during which morphologically stable dendrites emerge from the balancing of growth and retraction. Varying model parameters in biologically realistic ranges produces dendrite length and synapse density changes consistent with experiments. Our mechanistic model generates dendrites with approximately optimal wiring length, which is a widely used criterion for evaluating dendritic morphology (***Cuntz et al., 2010***, ***2012***; ***Chklovskii et al., 2002***). At the same time, the model leads to the activity-dependent emergence of functional synaptic organization and input selectivity. Therefore, our mechanistic modeling framework for the growth and stabilization of dendritic morphologies and the simultaneous synaptic organization according is ideally suited for making experimental predictions about the effect of perturbing specific model components on the resulting dendritic morphologies and synaptic placement.

Results

We built a computational model of activity-dependent dendrite growth during development based on synapse formation, stabilization, and elimination. We focused on basal stellate-like dendrites

of cortical pyramidal neurons, which primarily extend laterally within a layer of the cortex (***Larkman and Mason, 1990***) and receive numerous feedforward and recurrent inputs (***Rossi et al., 2019***; ***Iacaruso et al., 2017***). Stellate morphologies are found in many types of neurons, especially in the somatosensory cortex, including interneurons and layer 4 spiny stellate cells, which are the main recipients of thalamic inputs and play a key role in sensory processing (***Schubert et al., 2003***; ***Marques-Smith et al., 2016***; ***Scala et al., 2019***). To investigate the impact of synapse formation on dendrite development, we modeled several neuronal somata and potential synapses in a flat sheet of cortex (***Figure 1***a). Potential synapses represent locations in the cortex where an axon can form a synapse with a nearby dendrite (***Stepanyants and Chklovskii, 2005***). The model consists of two components: An activity-independent component that directly governs branch growth and retraction; and an activity-dependent component that governs synaptic organization and thus indirectly affects branch stability. Inspired by the synaptotrophic hypothesis (***Vaughn, 1989***), we mimicked the effect of activity-independent molecular signaling by letting each potential synapse release diffusive signaling molecules that attract the growing dendrite (***Figure 1***b, ***Figure 1–Figure Supplement 1***, ***Figure 1–Figure Supplement 2***). In addition, during development and before the onset of sensory experience, neural circuits generate patterned spontaneous activity (***Blankenship and Feller, 2010***; ***Ackman and Crair, 2014***). Therefore, to model the structured spontaneous activity exhibited by different axons (***Scholl et al., 2017***; ***Iacaruso et al., 2017***), we divided potential synapses randomly into different activity groups that receive inputs correlated within a group but uncorrelated between groups (see Methods). Each group represents either synapses from the same presynaptic neuron or from neurons that experience correlated presynaptic activity.

Because of their attraction to growth-factor releasing synapses and independent of neural activity, dendrites in our model grow outward from the soma towards the nearest potential synapse, where they form a synapse and temporarily stabilize (***Figure 1***b, ***Figure 1–Figure Supplement 2***). We assumed that dendrites could not overlap based on experimental data (***Grueber and Sagasti, 2010***); therefore, dendrites in the model retract, for instance, when further growth would require self-overlap. Once a synapse is formed, we modeled that its strength changes according to a local, activity-dependent plasticity rule (***Kirchner and Gjorgjieva, 2021***) (***Figure 1***c). The learning rule induces synaptic potentiation whenever presynaptic and local postsynaptic activity co-occur, and synaptic depression whenever local postsynaptic activity occurs in the dendrite independent of presynaptic stimulation, usually due to the activation of a neighboring synapse (see Methods and the 'offset' constant below),

$$\Delta\text{weight} = \text{post} \times (\text{pre} - \text{offset}). \tag{1}$$

As shown previously, this rule generates synaptic distance-dependent competition, where nearby synapses affect each other more than distant synapses, and correlation-dependent cooperation, where neighboring synchronized synapses stabilize. In contrast, neighboring desynchronized synapses depress (***Kirchner and Gjorgjieva, 2021***). In our model, we assumed that when a synapse depresses below a threshold, it decouples from the dendrite, and the corresponding branch retracts successively to either the nearest stable synapse, branch point, or the soma (***Figure 1***b, ***Figure 1–Figure Supplement 2***). After removal, the vacated synapse turns into a potential synapse again, attract-

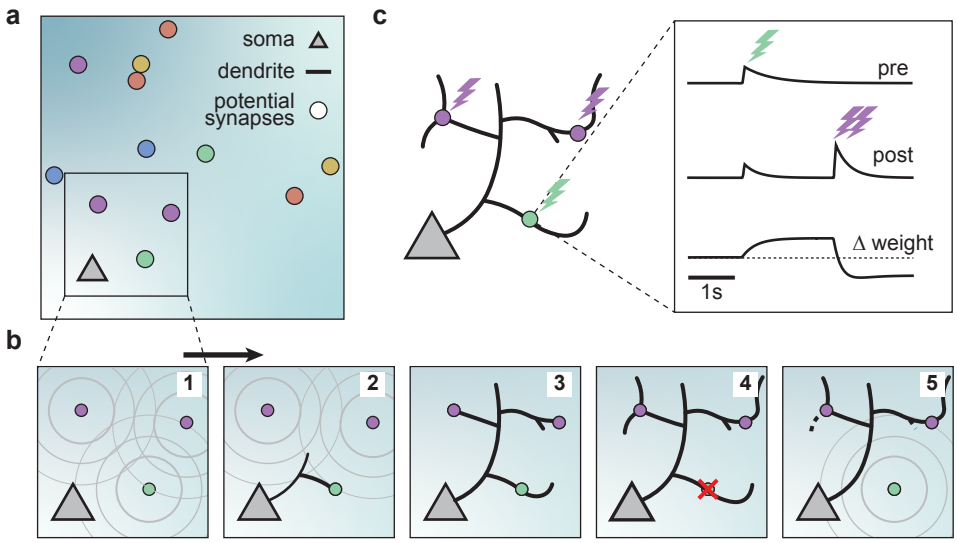

Figure 1. A model of dendritic growth for a cortical pyramidal neuron driven by activity-independent and -dependent mechanisms. (**a**) Schematic of the soma of a pyramidal neuron (orange triangle) with 12 randomly distributed potential synapses from presynaptic axons (circles) with correlated activity patterns indicated by color. (**b**) Schematic of activity-independent and -dependent mechanisms. Soma and synapses correspond to box in **a**. Signaling molecules diffusing from potential synapses (1) attract dendrite growth and promote synapse formation (2) independent of firing pattern (3). Over time, poorly synchronized synapses depress and are pruned from the dendrite (4), while well-synchronized synapses remain stable (5). After a branch retracts, the dendrite is less sensitive to the growth field at that location (5). (**c**) Change in weight of one synapse (green) following the stimulation of itself (green bolt) and of two nearby synapses (purple bolts). Left: Schematic of the developing dendrite from **b** with bolts indicating synaptic activation. Right: Presynaptic accumulator (top), postsynaptic accumulator (middle), and change in synaptic weight (bottom) as a function of time (see Methods ***Kirchner and Gjorgjieva*** (***2021***) for details of the plasticity rule). Dashed line (bottom) indicates zero change.

Figure 1–Figure supplement 1. The growth field is similar to two-dimensional heat diffusion.

Figure 1–Figure supplement 2. Detailed illustration of the dendritic growth mechanism.

ing other growing branches. Thus, a developing dendrite in our model acquires its arborization through the attraction to signaling molecules released by potential synapses and the repeated activity-dependent formation, stabilization and removal of synapses.

Dendrite development through balancing growth and retraction

After specifying the rules governing the growth of individual dendritic branches, we investigated dendritic development on long timescales. When growing dendrites according to our proposed growth rule based on signaling molecules attraction and spontaneous activity-dependent synaptic refinements (***Figure 1***), we found that dendrites form several stems, i.e. branches which start directly at the soma, and rapidly expand outwards (***Figure 2***a). After an initial phase of rapid expansion, we observed that growth rapidly attenuates, and the dendritic length stabilizes (***Figure 2***b). This stability is achieved when the dendrite's expansion and retraction are balanced (***Figure 2***c). To investigate whether the stability in total length also corresponds to stability in dendritic morphology, we quantified morphological stability as the pixel-wise correlation of a dendrite with itself 4.5 hours earlier, which is several orders of magnitude larger than the speed at which dendrites grow and retract in our model (see Table 1). Despite the residual amount of expansion and retraction, we showed that morphological stability increases rapidly, and the dendritic morphology is already stable after the initial expansion phase (***Figure 2***d). Interestingly, such rapid stabilization of morphology has also been observed in the mouse visual cortex (***Richards et al., 2020***) and the *Drosophila* larvae (***Castro et al., 2020***). We next quantified the Sholl diagram, the number of dendritic branches at a given distance from the soma, commonly used as a measure of dendritic complexity (***Sholl, 1953***; ***Binley et al., 2014***; ***Bird and Cuntz, 2019***). The Sholl diagram of the stabilized dendrites generated by our model is unimodal and qualitatively matches the Sholl diagram of developing basal dendrites from the mouse medial prefrontal cortex (***Figure 2***e; data extracted from ref. ***Kroon et al., 2019***, postnatal days 6-8), as well as the hippocampus (***Kleindienst et al., 2011***). In summary, by combining activity-independent and -dependent dendritic growth mechanisms, our model produces dendrites that rapidly expand and stabilize by balancing growth and retraction.

Delayed activity-dependent plasticity produces a rapid increase of synapse density followed by pruning

Since our model couples dendritic growth to the formation and removal of synapses (***Figure 3***a), we next investigated how the number of connected synapses, which are necessary for the dendrite's stabilization, changes over time. As a result of the dendrite's rapid growth, we observed a rapid increase in the number of connected synapses (***Figure 3***b,c). In contrast to the dendrite's length, we found that the initial rapid increase in connected synapses is followed by a brief period of an overall reduction of the number of synapses before additions and removals are balanced (***Figure 3***c). This removal of established synapses resembles the postnatal removal of synapses observed in the mouse neocortex (***Holtmaat et al., 2005***). To understand how the initial overshoot and subsequent removal of synapses emerge in our model, we computed the average synaptic weight of all synapses that eventually stabilize or are pruned (***Figure 3***d). We found that the delayed onset

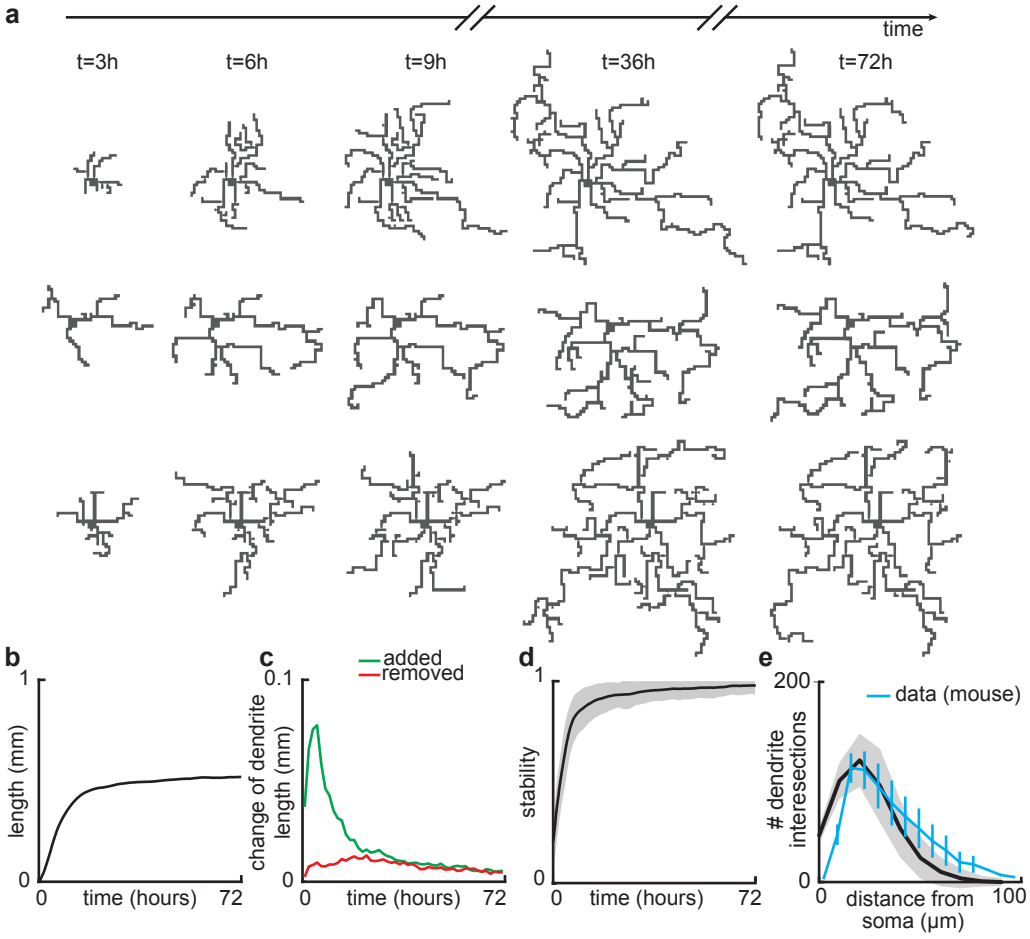

Figure 2. Balanced growth and retraction generate morphologically stable dendrites. (**a**) Three example dendrites at five time points from our simulations. For clarity of presentation, connected synapses are not displayed. (**b**) Total length of dendritic tree as a function of time. (**c**) Length of dendrite added (green) and removed (red) as a function of time. (**d**) Morphological stability (correlation between the dendrite shape at time t and $t - 4.5$ hours) as a function of time. (**e**) Average number of dendrite intersections as a function of distance from the soma (the Sholl diagram). Data from basal dendrites in the developing mouse medial prefrontal cortex superimposed, normalized to the maximum (blue; ref. (***Kroon et al., 2019***)). All lines represent averages across 32 simulations with nine dendrites each. Shaded area indicates two standard deviations.

Figure 2–video 1. Example of a simulation in which several dendrites develop in parallel.

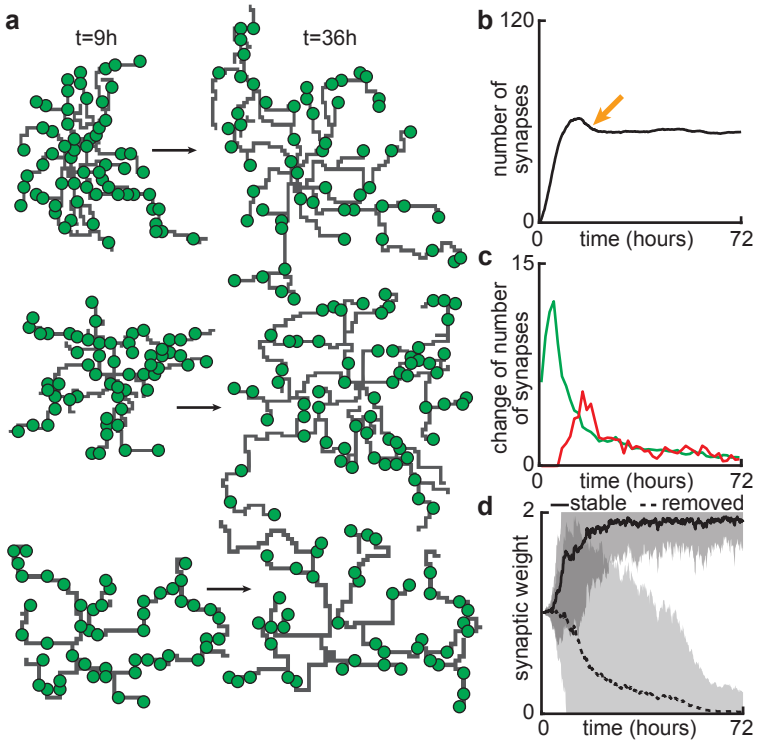

Figure 3. Synapse formation and removal predominate in distinct phases of dendrite development. (**a**) Three examples of dendrites at the beginning ($t = 9$ hours) and end (t =72 hours) of the simulation. Green circles indicate formed synapses. (**b**) Total number of connected synapses as a function of time. Orange arrow highlights overshoot and subsequent pruning. (**c**) Added (green) and pruned synapses (red) as a function of time. (**d**) Average synaptic weights of synapses that ultimately stabilize (solid black; final weight more than 0.5) or are removed (dashed black; final weight less than 0.5) as a function of time. All lines represent averages across 32 simulations with nine dendrites each. Shaded area indicates two standard deviations.

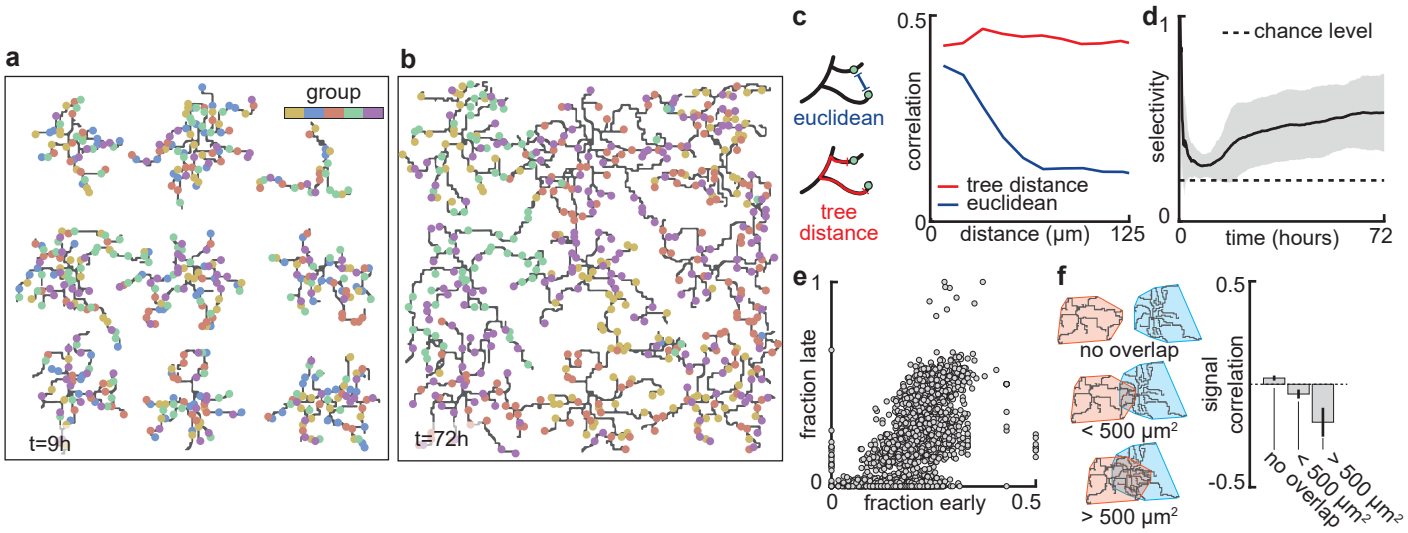

Figure 4. Stable morphology is obtained through selective removal of synapses and dendritic input selectivity. (**a**,**b**) Dendritic trees before (**a**, 9 hours) and after (**b**, 72 hours) removal of synapses (***Figure 3***). Connected synapses colored corresponding to activity group, which represents activity correlations (***Figure 1***b). (**c**) Left: Schematic illustrating the difference between Euclidean and tree distance. Note that we compute the Euclidean distance between synapses from different trees. Right: Correlation between pairs of synapses as a function of the Euclidean distance (blue) and tree distance (red). (**d**) Input selectivity of dendrites (defined as the fraction of the activity group with the highest representation) as a function of time. Dashed line indicates chance level. All lines represent averages across 32 simulations with nine dendrites each. Shaded area indicates two standard deviations. (**e**) Fraction of connected synapses per activity group early ($t = 9$ hours) and late ($t = 72$ hours) in the simulation. Each dot represents one of the five activity groups on one of the nine dendrites from the 32 simulations, resulting in $5 \times 9 \times 32 = 1440$ data points. (**f**) Left: Schematic of different levels of overlap (rows) between the convex hulls of two dendrites, referring to the smallest convex sets that contain the dendrite. Right: Signal correlation (correlation between fractions of synapses from the same activity groups) for different levels of dendritic overlap. Error bars indicate the standard error of the mean, computed from 1152 pairs of dendrites from 32 simulations.

of synapse removal (***Figure 3***c) is due to the slow time scale of the synaptic weight compared to the faster time scale of dendrite growth. Thus, the initial overshoot and subsequent removal of synapses observed in our model (***Figure 3***b) is due to the rapid formation relative to the delayed activity-dependent elimination of synapses.

Activity-dependent competition between synapses produces input selectivity and synaptic organization

Next, we asked if the stabilization of dendrites might be supported by the emergence of organization of connected synapses. First, we compared the synapses connected to dendrites at the apex of the overshoot phase (peak in ***Figure 3***b) with those in the stabilization phase (***Figure 4***a,b). While dendrites at the apex do not prefer synapses from any particular input group, in the stabilization phase, they acquire a preference for synapses from only two or three of the activity groups (***Figure 1***b). These dynamics resemble the activity-dependent synaptic competition in the developing visual cortex, where asynchronously activated synapses tend to depress (***Winnubst et al., 2015***). Notably, the remaining synchronized synapses in our model experience correlation-dependent cooperation (***Kirchner and Gjorgjieva, 2021***), and are therefore able to stabilize the dendrite and prevent the total retraction of all branches.

This selective potentiation of synapses according to input correlation also leads to dendritic selectivity for inputs. In particular, synapses on the same dendrite are likely to come from the same activity group (***Figure 4***c). This selectivity is acquired throughout the simulation, where selectivity starts high (a nascent dendrite is trivially selective to its first synapse; $t = 0-1$ hours), drops almost to chance level (indiscriminate addition of synapses; $t = 9$ hours), and finally approaches a value of $\frac{1}{2}$ (two activity groups per dendrite remain after the pruning phase; $t = 72$ hours) (***Figure 4***d). To determine which activity group stabilizes eventually, we computed selectivity for each group early ($t = 9$ hours) and late ($t = 72$ hours). We found that early high (low) selectivity for an activity group translates into even higher (lower) selectivity in the stable state (***Figure 4***e), predicting an outsized impact of early synaptic contacts on continued dendritic function. Finally, we observed that when dendritic trees overlap strongly, they tend to be selective to different activity groups (***Figure 4***f) due to competition for limited potential synapses of any given group. Interestingly, also in the mouse visual cortex, neighboring neurons often exhibit different selectivity (***Ohki et al., 2005***), potentially reflecting a lasting impact of early competition between different inputs.

In summary, the emergence of dendrites' selectivity for synapses from specific activity groups coincides with and supports the stabilization of dendritic morphologies.

Balance of mature and immature brain-derived neurotrophic factor controls arborization of dendrites

After establishing that our model can capture some important aspects of the dynamics of dendritic development through the combination of activity-independent and activity-dependent mechanisms, including local plasticity, we asked how changing properties of the plasticity rule might affect dendritic growth and synaptic organization. Developmentally, the interaction between two neurotrophic factors, BDNF and proBDNF (***Figure 5***a), has been found to play a key role in organization of synaptic inputs into clusters (***Niculescu et al., 2018***). Therefore, through the previously established link between this neurotrophin interaction and synaptic plasticity (***Kirchner and Gjorgjieva, 2021***), we investigated the influence of changing the underlying molecular interactions on dendritic morphology.

As we have previously shown, the "offset" term in our plasticity rule (***Equation 1***) represents the neurotrophin balance (computed as BDNF/(BDNF+proBDNF)) released upon stimulation of a synapse (***Kirchner and Gjorgjieva, 2021***). Consequently, we found that an overabundance of BDNF (proBDNF) leads to potentiation (depression) of the synapse (***Figure 5***b), consistent with experimental data (***Lu et al., 2005***). Furthermore, our plasticity rule acts locally on the dendrite so that the strength of individual synapses is affected by interactions with other nearby synapses. Concretely, a lower (higher) density of nearby synapses tends to lead to potentiation (depression) of the synapse (***Kirchner and Gjorgjieva, 2021***).

To better understand the interactions between the balance of neurotrophins and the density of synapses, we analytically derived the maximum density of synapses that can stabilize given a balance of neurotrophins (***Figure 5***c, see Methods). We found that an overabundance of BDNF (proBDNF) leads to a higher (lower) maximal density of synapses (***Figure 5***c). Indeed, when we simulated dendritic development with varying neurotrophin ratios, we found that the density of

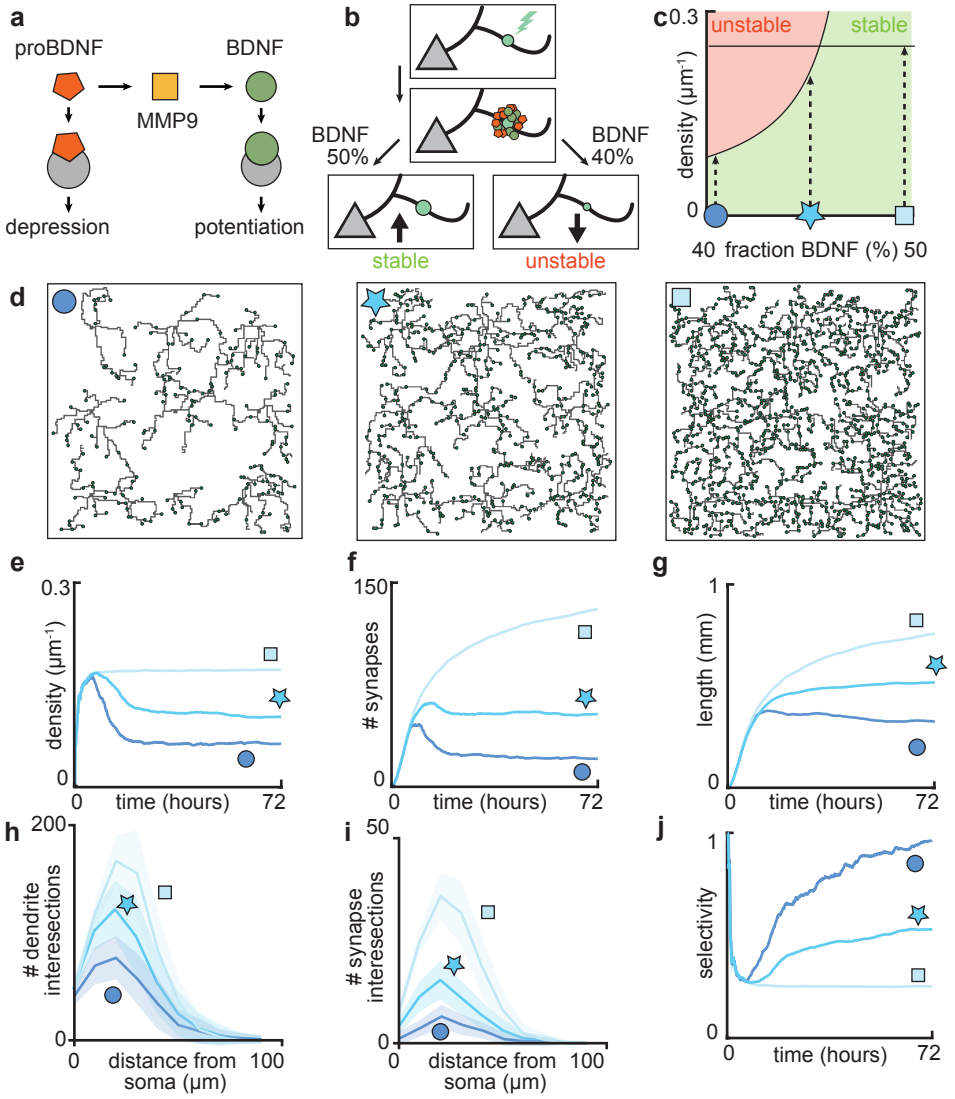

Figure 5. Dendritic arborization is controlled by the ratio of neurotrophic factors. (**a**) Interactions between molecular factors underlie a local activity-dependent plasticity rule for synaptic change (***Equation 1***, (***Kirchner and Gjorgjieva, 2021***)). Neurotrophins (BDNF and proBDNF) bind to different neurotrophin receptors, and a cleaving protease (MMP9) converts proBDNF to BDNF in an activity-dependent manner. (**b**) Schematic illustrating the impact of different concentrations of BDNF on synaptic change. Upon stimulation of a synapse (top), proBDNF and BDNF is released into extracellular space (middle), where proBDNF can be cleaved into BDNF by MMP9. Depending on the neurotrophin ratio, computed as BDNF/(BDNF + proBDNF), the synapse is stabilized (left) or depressed and hence eventually removed (right). (**c**) Maximally possible stable density of synapses as a function of the initial concentration of BDNF. Stable (no pruning; green) and unstable (pruning occurs; red) areas are indicated. (**d**) Three examples of dendrites with superimposed synapses (green) with high initial BDNF concentration (49%), the baseline concentration (45%, same as ***Figure 1-Figure 3***) and low initial BDNF (40%). Symbols correspond to locations marked in panel c. (**e-g**) Averages for density of synapses on the dendrite (**e**), number of connected synapses (**f**) and total length of dendrite (**g**) as a function of time for dendrites from the three conditions shown in **d**. (**h-i**) Average number of dendrite intersections (**h**) and synapses (**i**) as a function of distance from the soma for dendrites from the three conditions shown in **d**. (**j**) Global selectivity as a function of time for dendrites from the three conditions shown in **d**. All lines represent averages across 32 simulations with nine dendrites each.

synapses per dendrite increases with increasing neurotrophin ratio (***Figure 5***d,e). Consistent with biological evidence (***McAllister et al., 1995***; ***Tyler and Pozzo-Miller, 2001***), in our model, developing dendrites treated with BDNF tend to grow larger and have a higher density of synapses (***Figure 5***e,g). In contrast, over-expression of proBDNF leads to smaller dendrites with fewer synapses (***Koshimizu et al., 2009***; ***Yang et al., 2014***) (***Figure 5***f,g). Perturbing the balance between neurotrophins scales the Sholl diagram of dendrite intersections and synapses, but does not qualitatively affect the shape of the curve (***Figure 5***h,i).

In our model, these changes in length and density are explained by a change in selectivity of synapses (***Figure 5***j). Concretely, an increase in BDNF erases all synaptic competition, reducing the selectivity to chance level, while an increase in proBDNF greatly amplifies synaptic competition and thus selectivity. These differences in competition determine the number of pruned synapses and thus the length at which the dendrite stabilizes. Thus, our model predicts that biologically-relevant differences in dendritic morphology may arise from different neurotrophin ratios due to the maximal density of synapses that stabilizes the dendrite.

Different impacts of activity-dependent and -independent factors on dendritic development

Our mechanistic model enabled us to dissect the different roles of activity-dependent and -independent mechanisms on dendritic morphology. To this end, we varied either only activity-dependent factors or only activity-independent factors across a set of simulations (***Figure 6***a). We introduced variability in the activity-dependent aspects of the model through the firing patterns of potential synapses, and in the activity-independent aspects of the model via fluctuations in both the extrinsic growth signals and the intrinsic mechanisms underlying dendrite growth (see Methods, ***Figure 6***b).

Consistent with experiments (***Scala et al., 2021***), dendrites produced by our model exhibit substantial variability in morphology (***Figure 6***a), length (***Figure 6***c), and number of synapses (***Figure 6***d). Comparing dendrites that experienced either identical activity-dependent or -independent factors allowed us to compute the percentage of change in morphology attributable to each factor as a function of developmental time (***Figure 6***e,f). We found that while activity-independent factors tend to lead to large differences in morphology early on, activity-dependent factors affect dendrite morphology with a substantial delay. These differences can be explained by the delay in synaptic pruning relative to initial synaptic formation (***Figure 3***d).

Despite substantial variability, there are predictive factors for the final length of the dendrite. In particular, we found a positive relationship between the number of major branches, i.e. branches starting from the soma, and the final length (***Figure 6***g). Interestingly, this is consistent with reconstructed dendrites from multiple regions of the mouse cortex (***Figure 6–Figure Supplement 1***). Furthermore, our model predicts that dendrites that have a high (low) total length early on will, on average, retain a (high) low total length throughout development (***Figure 6***e).

Thus, our model suggests that while activity-independent factors affect dendritic morphology early on during development, activity-dependent factors dominate later. Properties like the number of major branches or the length of dendrites during early development might be predictive of the dendrite's morphology throughout the animal's lifetime.

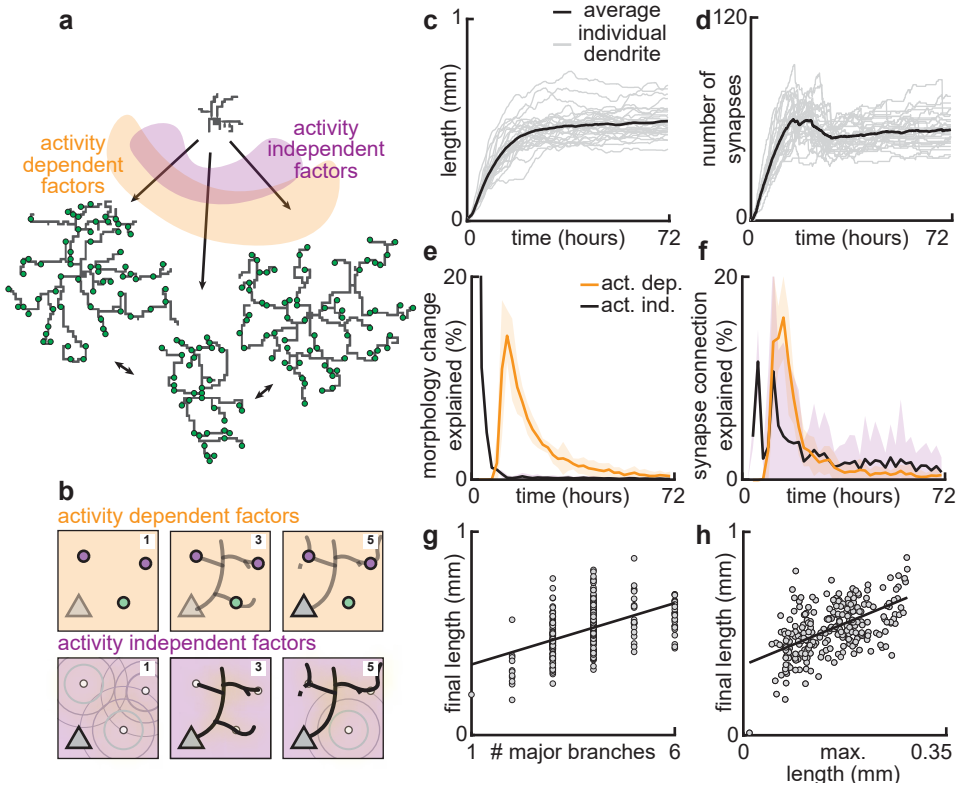

Figure 6. Morphological variability emerges from the interaction of activity-dependent and -independent factors. (**a**) Example of three dendrites with identical initial conditions but different random seeds. The colors illustrate that initial growth is governed by activity-independent factors, while later growth is governed by activity-dependent factors. (**b**) Schematic illustrating how variability is introduced into model: activity-dependent via the patterns of spontaneous activity (orange), and activity-independent via fluctuations in both the extrinsic growth stimulating field (purple 1) and the intrinsic mechanisms underlying dendrite growth (purple 2; see Methods). (**c,d**) Total length (**c**) and number of synapses (**d**) as a function of time for dendrites with identical initial conditions but different random seeds. Each gray line corresponds to one dendrite from one of 32 simulations. Bold line represents average. (**e,f**) Percentage in change of morphological similarity (**e**) and similarity of connected synapses (**f**) as a function of time for simulations where activity-dependent (orange) or -independent (purple) factors vary. Lines represent averages across 32 simulations with nine dendrites each. Shaded area indicates two standard deviations. (**g,h**) Final length as a function of number of major branches (**g**) and maximal length in the first 18 hours of the simulation (**h**). Lines indicate linear regression.

Figure 6–Figure supplement 1. Total tree length increases with the number of stems.

Coupled dendrite growth and synapse formation leads to approximately optimal wiring

Since space is limited in the cortex and maintaining complex morphologies is costly, it is beneficial for a neuron to connect to its synapses with the minimum possible dendrite length (***Cuntz et al., 2012***) (***Figure 7***a). In our model, dendrites are assumed to grow towards the nearest potential synapse. Thus, we investigated how the final length in our model compares to the optimal wiring length. The optimal length (L) of dendrites in a plane scales with the square root of the number of synapses (N) times the area over which the synapses are distributed (A): $L = \sqrt{NA/\pi}$ (***Cuntz et al., 2012***). In contrast, the length of a dendrite when synapses are connected randomly scales with the number of connected synapses times the average distance of two random points on a circle (***Uspensky, 1937***), $L = N\frac{128}{45\pi}\sqrt{A/(2\pi)}$ which differs from the optimal result by a square root in the number of synapses. Using the convex hull that circumscribes the stabilized synapses as the area over which the synapses are distributed (***Figure 7***b), we compared the actual dendrite length with the optimal and the random wiring length (***Figure 7***c). We found that our simulated dendritic lengths are shorter than random wiring and longer than the theoretical optimal length.

We next wanted to know if the deviation from optimality might quantitatively match the one observed in real dendrites. To investigate this question, we reanalyzed a published dataset (***Cuntz et al., 2012***) containing the total lengths and the number of branch points of 13,112 dendrites pooled across 74 sources. When computing the fold change between the real and the optimal dendritic length in the dataset, we confirmed that real dendrites tend to be consistently larger than the theoretical optimum (***Figure 7***d). Interestingly, the fold change between the length of real dendrites and the theoretical optimum is similar to the fold change of our simulated dendrites and the theoretical optimum (***Figure 7***e). This deviation is expected given the heterogeneous structure of neuronal tissue that hampers diffusion of signaling molecules (***Nicholson et al., 2000***; ***Motta et al., 2019***), which mirrors the fluctuations in activity-independent factors in our model. Therefore, activity-dependent dendrite growth produces morphologies with a total length close to the theoretically possible minimum.

Discussion

Dendrite growth and the formation, stabilization and removal of synapses during early development depend on various factors during development, including extrinsic factors such as growth cues, intrinsic molecular signaling, and correlated patterns of spontaneous activity, but the nature of these interactions and the implications for dendritic function throughout life remain largely unexplored. In this study, we proposed a mechanistic model for the growth and retraction of dendritic branches as well as the formation and removal of synapses on these dendrites during development, based on the interaction of activity-independent cues from potential synaptic partners and local activity-dependent synaptic plasticity. Our model can simultaneously capture two main aspects of dendritic growth: produce dendritic morphologies and drive synaptic organization.

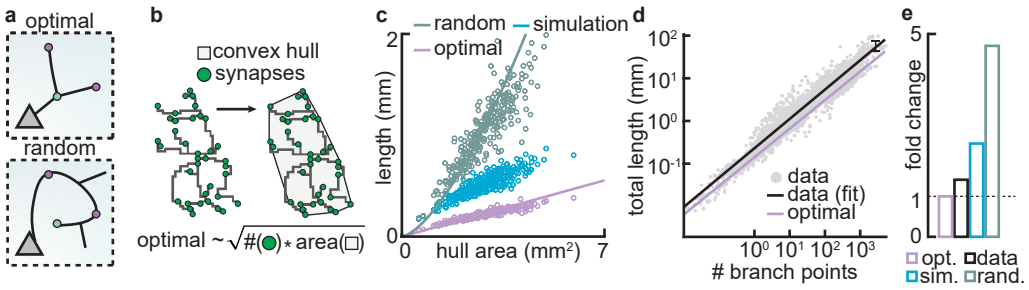

Figure 7. Dendritic morphology approximately minimizes cable length. (**a**) Schematic illustrating optimal (top) and random (bottom) wiring to connect a given set of synapses. (**b**) The convex hull of all synapses connected to a dendrite with the proportionality of optimal length (bottom). (**c**) Total tree length as a function of convex hull area in the optimal, simulated and random scenario. Each dot corresponds to one of 288 dendrites from 32 simulations. Lines correspond to analytic predictions for the average density across all simulations. (**d**) Total tree length against the number of branch points in log scale, both for data and theoretical optimum. Data extracted from (***Cuntz et al., 2012***). (**e**) Total tree length in the data (black, average of n=13,112), our simulations (blue, average of 288 dendrites from 32 simulations), and the random baseline (green, analytically computed) relative to theoretical optimum (pink, analytically computed).

Assumptions and predictions of the model

Some of the most prominent models of dendritic growth have focused on activity-independent rules based on geometric or biophysical constraints (***Cuntz et al., 2010***, ***2012***). Despite their immense success in generating realistic dendritic morphologies, they leave open the question of the underlying biological mechanisms. Other studies have implemented global activity-dependent rules that require feedback signals from the soma or the axon (***Ooyen et al., 1995***). Our model proposes a simple and biologically plausible mechanism for the simultaneous dendritic growth and synaptic organization based on activity-independent cues and local activity-dependent learning rules, which cluster synaptic inputs according to functional preferences. Numerous experimental studies have demonstrated the importance of such local plasticity for the emergence of local synaptic organization in the form of clusters as well as dendritic function (***Hering and Sheng, 2001***; ***Lohmann et al., 2002***; ***Chen et al., 2013***; ***Niculescu et al., 2018***).

Our model makes some simplifying assumptions at the expense of mechanistic insights. For instance, we model the generation of only stellate-like morphologies without the apical trunk. Many types of neurons are characterized by stellate morphologies, especially in the somatosensory cortex (***Schubert et al., 2003***; ***Marques-Smith et al., 2016***; ***Scala et al., 2019***). Nonethless, it would be interesting to investigates if our model's mechanisms can be minimally modified to apply to the generation of apical dendrites. Moreover, we generate our model dendrites in a two-dimensional, flat sheet of cortex. We anticipate that the models can be straightforwardly extended to three dimensions, but with additional computational cost. Although our assumptions may be too simplified to generate perfectly biologically realistic morphologies, the simple rules in our model capture basic morphological features, such as the number of branches, the total length, and the Sholl analysis, with those of biological neurons reported in the literature.

A key advantage of our mechanistic model is the ability to predict the impact of early perturbations on mature dendritic morphology, as the model allows us to independently investigate

activity-independent and -dependent influences on dendrite growth and synaptic organization. For example, three distinct phases of synapse development – overshoot, pruning, stabilization – and stable dendritic trees emerge naturally from the interactions between activity-independent signaling and the activity-dependent synaptic plasticity, without additional assumptions. The stabilization of dendritic morphologies in our model is enabled by the emergence of input selectivity, which implies local organization of synapses responsive to a particular correlated input pattern on the dendrite. Hence, our model explains how dendritic morphology can adapt to changes in the activity-dependent plasticity or the input statistics during development, as observed experimentally (***Cline and Haas, 2008***; ***McAllister et al., 1995***; ***Tyler and Pozzo-Miller, 2001***). Further, we provide a mechanistic explanation for the emergence of approximately optimal wiring length in mature dendrites. Thus, our model provides a new perspective on the interaction of activity-independent and -dependent factors influencing dendrite growth and suggests that the formation and activity-dependent stabilization vs. removal of synapses might exert powerful control over the growth process.

Comparison with the synaptotrophic hypothesis

The synaptotrophic hypothesis, originally proposed three decades ago (***Vaughn, 1989***), has provided a useful framework for interpreting the effect of neural activity and synapse formation on dendrite development. Our proposed model is inspired by the synaptotrophic hypothesis but differs from it in a few key aspects. (1) The synaptotrophic hypothesis postulates that synaptic activity is necessary for dendrite development (***Cline and Haas, 2008***). In contrast, our model contains an activity-independent component that allows dendrites to grow even in the absence of synaptic activity. Our model is thus consistent with the finding that even in the absence of neurotransmitter secretion connected neuronal circuits with morphologically defined synapses can still be formed (***Verhage et al., 2000***) and with computational (non-mechanistic) models that produce dendrites with many relevant morphological properties without relying on activity (***Cuntz, 2016***). (2) The synaptotrophic hypothesis does not specify the exact molecular factors underlying the information exchange pre- and postsynaptically. Informed by recent experiments that identify central molecular candidates (***Winnubst et al., 2015***; ***Kleindienst et al., 2011***; ***Niculescu et al., 2018***; ***Lu et al., 2005***), our model proposes a concrete mechanistic implementation based on neurotrophic factors (***Kirchner and Gjorgjieva, 2021***). (3) The synaptotrophic hypothesis postulates that whether a potential synaptic contact is appropriate can be rapidly evaluated pre- and postsynapically. Inspired by experiments (***Lohmann et al., 2002***; ***Niell et al., 2004***), the fate of a synapse in our model is determined only within tens of minutes or hours after it is formed. This is due to the slow timescale of synaptic plasticity (***Figure 3***d).

Relationship between dendritic form and function

While previous studies focused on how dendritic morphology affects function, e.g. through nonlinear signal transformation (***Poirazi and Papoutsi, 2020***) or dynamic routing of signals (***Payeur et al., 2019***), we propose that dendrite form and function reciprocally shape each other during development. While the dendrite's morphology constrains the pool of available potential synapses, synap-

tic activity determines the dendritic branch's stability (Fig. 1). As a result, the dendritic tree self-organizes into an appropriate shape to support a limited number of functionally related synapses. These initial synaptic contacts might then serve as a scaffold around which additional, functionally related synapses cluster to form the building blocks to support the powerful computations of mature dendrites (***Kirchner and Gjorgjieva, 2022***).

Dynamics of dendritic development

Here we focus on the early developmental period of highly dynamic dendritic growth and retraction. However, dendritic morphology remains remarkably stable in later development and throughout adulthood (***Richards et al., 2020***; ***Castro et al., 2020***; ***Koleske, 2013***). This stability is achieved despite substantial increases in overall size of the animal (***Richards et al., 2020***; ***Castro et al., 2020***) and ongoing functional and structural plasticity of synapses (***Kleindienst et al., 2011***; ***Winnubst et al., 2015***; ***Kirchner and Gjorgjieva, 2021***). While it is still unclear how exactly synaptic organization is established during early development and how synapses are affected by the overall increase in dendrite size, somatic voltage responses to synaptic activity are largely independent of dendrite size (***Cuntz et al., 2021***). It has been shown that dendrite stability plays a crucial role in enabling the correct function of the adult brain and is disrupted in many psychiatric disorders and neurodegenerative diseases. In particular, the release of BDNF, which is connected to synaptic activity, affects structural consolidation of dendrites and, thus, long-term stability (***Koleske, 2013***). Our mechanistic model allows us to perturb the balance of neurotrophic factors and investigate the effects on dendritic development. For instance, our model predicts detrimental effects on dendrite stability as a result of extreme or non-existent input selectivity, providing insight into functional consequences of disrupted dendrite growth in neurodevelopmental disorders (***Johnston et al., 2016***).

Interneurons and inhibitory synapses

In addition to excitatory neurons and synapses that are the focus of this study, inhibitory interneurons and inhibitory synapses also play an important role in brain development (***Naskar et al., 2019***). Interneurons fall into genetically-distinct subtypes, which tend to target different portions of pyramidal neurons (***Rudy et al., 2011***; ***Kepecs and Fishell, 2014***). In particular, somatostatin-expressing (SST) interneurons preferentially target the dendrites of pyramidal neurons, while parvalbumin-expressing (PV) interneurons preferentially target the soma. Furthermore, the dendrites of inhibitory neurons have a complex morphology that likely allows them to perform intricate transformations of incoming signals (***Tzilivaki et al., 2019***, ***2021***). Investigating whether and how inhibitory interneurons and synapses might interact with excitatory ones during dendritic development is an exciting direction for future research.

In summary, by proposing a mechanistic model of dendritic development which combines activity-independent and -dependent components, our study explains several experimental findings and makes predictions about the factors underlying variable dendritic morphologies and synaptic organization. Interestingly, the stable morphologies it generates are approximately optimal in terms of

wiring length and experimental data. Finally, our model provides the basis for future exploration of different learning rules and cell types which could differ across brain regions, species and healthy vs. disease states.

Methods and Materials

Activity-independent synaptic signals. In the synaptotrophic hypothesis, dendrite growth is directed towards potential synaptic partners. In our model, we capture this aspect by introducing a *growth field* of activity-independent synaptic signals, $\mathrm{T}(\mathbf{p})$, over all positions $\mathbf{p}$ in our sheet of cortex. This field contains point sources at the positions of potential synapses, $\mathbf{p}_i$, and evolves over time according according to a diffusion equation,

$$\mathrm{T}(\mathbf{p})^{t+1} = \mathrm{T}(\mathbf{p})^{t} * \mathrm{D} + \mu \sum_i \mathbf{p}_i + \sigma \mathbf{N}. \tag{2}$$

The growth field at time point $t+1$ is therefore given by the sum of the growth field at time t convolved with a diffusion filter D, a constant input of size μ from all potential synapses, which are currently not connected to a dendrite, as well as independent Gaussian noise, $\mathbf{N}$, with standard deviation σ. We chose a two dimensional Gaussian for the diffusion filter D, making the field $\mathrm{T}(\mathbf{p})$ mathematically equivalent to a heat diffusion in two dimensions (***Figure 1–Figure Supplement 1***).

Asynchronous dendrite growth and retraction. Dendrite development critically depends on resources from the soma (***Ye et al., 2007***). Consequently, we modeled the growth of dendrites to depend on *scouting agents* that spread outward from the soma at regular time intervals, t_{scout}, and that traverse the dendritic tree at speed v_{scout} (***Figure 1–Figure Supplement 2***). These scouting agents resemble actin-blobs that control dendrite growth (***Nithianandam and Chien, 2018***). When a scouting agent encounters a branch point, there is a 0.5 chance for it to continue in any direction. This means it can go in one direction, but it can also duplicate or disappear completely. We further model these scouting agents to detect the growth field's value – a scouting agent stops at a position on the dendrite where this field is locally maximal and marks this location for growth. The dendrite will then expand at the marked positions in the direction of the gradient of the growth field, and the scouting agent moves to this new position. If the dendrite grows to the location of a potential synapse, this synapse is then realized, and its initial weight is set to $w_{init} = \frac{1}{2}$. Two branches of the same neuron may never become adjacent; however, branches from other neurons may be crossed freely. If a scouting agent reaches the end of a branch without finding a local maximum of the growth field along its path, the scouting agent initiates the retraction of this branch. Depending on proximity, a branch then retracts up to the nearest stable synapse, the next branch point, or the soma. Because our simulations are a spatially discrete approximation of a biological flat sheet of cortex, we had to ensure that growth behaves appropriately in cases where the discretization scheme becomes relevant (***Figure 1–Figure Supplement 2***).

Minimal plasticity model. When a synapse k forms on the dendrite, its weight w_k evolves according to a previously proposed minimal plasticity model for interactions between synapses on developing dendrites (***Kirchner and Gjorgjieva, 2021***). This model can be linked to a full neurotrophin model that interprets the parameters in terms of the neurotrophic factors BDNF, proBDNF, and

the protease MMP9. In this model, the k-th synapse is stimulated within input event trains x_k

$$x_k(t) = \int_0^\infty \sum_f \delta(s - s_k^f)(H(t-s) - H(t - x_{\text{dur}} - s))\mathrm{d}s \tag{3}$$

with events at times t_k^f and where the Heaviside step function $H(t)$ is 0 when t is less than 0 and 1 when t is greater or equal than 0, so that events have duration x_{dur} (50 time steps). The minimal plasticity model consists of a synapse-specific presynaptic accumulator v_k,

$$\tau_v \frac{\mathrm{d}v_k}{\mathrm{d}t} = -v_k(t) + \phi x_k(t), \tag{4}$$

and a postsynaptic accumulator u_k that averages over nearby synapses in a weighted and distance-dependent manner,

$$\tau_u \frac{\mathrm{d}u_k}{\mathrm{d}t} = -u_k(t) + \sum_{l=1}^{N} s_{kl} w_l(t) x_l(t). \tag{5}$$

The multiplicative factor ϕ is an MMP9 efficiency constant that determines how efficiently MMP9 converts proBDNF into BDNF per unit of time and the proximity variables s_{kl} between synapses k and l on the same dendrite are computed as $s_{kl} = e^{-\frac{d_{kl}^2}{2\sigma_s^2}}$, where σ_s determines the spatial postsynaptic calcium spread constant. The equation governing the weight development of w_k (***Equation 6***) is a Hebbian equation that directly combines the pre- and postsynaptic accumulator with an additional offset constant ρ,

$$\tau_w \dot{w}_k = u_k(t)(v_k(t) + \rho), \tag{6}$$

with $\rho = \frac{2\eta - 1}{2(1-\eta)}$ and $\tau_w = \tau_W \frac{1}{2(1-\eta)}$. Here, η is the constitutive ratio of BDNF to proBDNF and $\tau_W = 3000\,\text{ms}$ This model is minimal in the sense that it cannot be reduced further without losing either the dependence on correlation through the link to the BTDP rule, or the dependence on distance.

To model structural plasticity, we implemented a structural plasticity rule inspired by ref. (***Holtmaat and Svoboda, 2009***) where each synapse whose efficacy falls below a fixed threshold W_{thr} is pruned from the dendrite.

Simulations and parameters. For all simulations in this study, we distributed nine somata at regular distances in a grid formation. We used 1500 potential synapses and divided them into five groups of equal size, with each group receiving Poisson input with rate r_{in}. Therefore, all synapses in the same group are perfectly correlated, while synapses in different groups are uncorrelated.

Acknowledgments

This work was supported by the Max Planck Society and the European Research Council (ERC) under the European Union's Horizon 2020 research and innovation program (Grant agreement No. 804824).

Competing interests

No competing interests declared.

Table 1. Parameters of the minimal plasticity model (***Kirchner and Gjorgjieva, 2021***) and the synaptotrophic growth model.

Parameter	Variable	Value
Synaptic efficacy time constant	τ_W	6000 time steps
Postsynaptic accumulator time constant	τ_u	300 time steps
Presynaptic accumulator time constant	τ_v	600 time steps
Constitutive percent of BDNF of total neurotrophins	η	45%
MMP9 efficiency constant	ϕ	$\frac{3}{50}$ per time step
Heterosynaptic offset	ρ	$\rho = \frac{2\eta-1}{2(1-\eta)}$
Minimal model synaptic efficacy time constant	τ_w	$\tau_w = \tau_W \frac{1}{2(1-\eta)}$
Standard deviation of calcium spread	σ_c	$200\,\mu m$
Turnover threshold below which a synapse is replaced	W_{thr}	0.02
Firing rate of synapses	r_{in}	$0.116\,\text{min}^{-1}$
Scout intervals and speed	t_{scout}, v_{scout}	$10\,\text{min}, 0.18\,\mu m\,\text{min}^{-1}$

References

Ackman JB, Crair MC. Role of emergent neural activity in visual map development. Current opinion in neurobiology. 2014; 24:166–175.

Binley KE, Ng WS, Tribble JR, Song B, Morgan JE. Sholl analysis: a quantitative comparison of semi-automated methods. J Neurosci Methods. 2014; 225:65–70.

Bird A, Cuntz H. Dissecting Sholl Analysis into Its Functional Components. Cell Reports. 2019; 27:3081–3096.

Blankenship AG, Feller MB. Mechanisms underlying spontaneous patterned activity in developing neural circuits. Nature Reviews Neuroscience. 2010; 11(1):18–29.

Campbell G, Ramoa AS, Stryker MP, Shatz CJ. Dendritic development of retinal ganglion cells after prenatal intracranial infusion of tetrodotoxin. Visual neuroscience. 1997; 14(4):779–788.

Castro AF, Baltruschat L, Stürner T, Bahrami A, Jedlicka P, Tavosanis G, Cuntz H. Achieving functional neuronal dendrite structure through sequential stochastic growth and retraction. Elife. 2020; 9:e60920.

Chen TW, Wardill T, Sun Y, R PS, Renninger SL, Baohan A, Schreiter ER, Kerr RA, Orger MB, Jayaraman V, Looger LL, Svoboda K, Kim DS. Ultrasensitive fluorescent proteins for imaging neuronal activity. Nature. 2013; 499:295–300.

Chklovskii DB, Schikorski T, Stevens CF. Wiring optimization in cortical circuits. Neuron. 2002; 34(3):341–347.

Cijsouw T, Weber JP, Broeke JH, Broek JA, Schut D, Kroon T, Saarloos I, Verhage M, Toonen RF. Munc18-1 redistributes in nerve terminals in an activity-and PKC-dependent manner. Journal of cell biology. 2014; 204(5):759–775.

Cline H, Haas K. The regulation of dendritic arbor development and plasticity by glutamatergic synaptic input: a review of the synaptotrophic hypothesis. The Journal of physiology. 2008; 586(6):1509–1517.

Cline HT. Experience-dependent dendritic arbor development. In: *Dendrites: Development and Disease* Springer Japan; 2016.p. 295–315. doi: 10.1007/978-4-431-56050-013.

Crair MC. Neuronal activity during development: permissive or instructive? Current opinion in neurobiology. 1999; 9(1):88–93.

Cuntz H. Modeling dendrite shape. In: *Dendrites* Oxford University Press; 2016.p. 487–504. doi: 10.1093/acprof:oso/9780198745273.003.0017.

Cuntz H, Bird AD, Mittag M, Beining M, Schneider M, Mediavilla L, Hoffmann FZ, Deller T, Jedlicka P. A general principle of dendritic constancy: A neuron's size-and shape-invariant excitability. Neuron. 2021; 109(22):3647–3662.

Cuntz H, Forstner F, Borst A, Häusser M. One Rule to Grow Them All: A General Theory of Neuronal Branching and Its Practical Application. PLoS Computational Biology. 2010 aug; 6(8):e1000877. doi: 10.1371/journal.pcbi.1000877.

Cuntz H, Mathy A, Häusser M. A scaling law derived from optimal dendritic wiring. Proceedings of the National Academy of Sciences. 2012; 109(27):11014–11018.

Gouwens N, Sorensen S, Baftizadeh F, Budzillo A, Lee B, Jarsky T, Alfiler L, Arkhipov A, Baker K, Barkan E, Berry K, Bertagnolli D, Bickley K, Bomben J, Braun T, Brouner K, Casper T, Crichton K, Daigle T, Dalley R, et al. Toward an Integrated Classification of Cell Types: Morphoelectric and Transcriptomic Characterization of Individual GABAergic Cortical Neurons. SSRN Electronic Journal. 2020 feb; p. 2020.02.03.932244. https://doi.org/10.1101/2020.02.03.932244, doi: 10.1101/2020.02.03.932244.

Grueber WB, Sagasti A. Self-avoidance and tiling: mechanisms of dendrite and axon spacing. Cold Spring Harbor perspectives in biology. 2010; 2(9):a001750.

Haas K, Li J, Cline HT. AMPA receptors regulate experience-dependent dendritic arbor growth in vivo. Proceedings of the National Academy of Sciences of the United States of America. 2006 aug; 103(32):12127–12131. doi: 10.1073/pnas.0602670103.

Hering H, Sheng M. Dendritic spines: structure, dynamics and regulation. Nature Reviews Neuroscience. 2001; 2(12):880–888.

Holtmaat A, Svoboda K. Experience-dependent structural synaptic plasticity in the mammalian brain. Nature Reviews Neuroscience. 2009; 10(9):647.

Holtmaat AJ, Trachtenberg JT, Wilbrecht L, Shepherd GM, Zhang X, Knott GW, Svoboda K. Transient and persistent dendritic spines in the neocortex in vivo. Neuron. 2005; 45(2):279–291.

Iacaruso FM, Gasler IT, Hofer SB. Synaptic organization of visual space in primary visual cortex. Nature. 2017; 547(7664):449–452.

Je HS, Yang F, Ji Y, Nagappan G, Hempstead BL, Lu B. Role of pro-brain-derived neurotrophic factor (proBDNF) to mature BDNF conversion in activity-dependent competition at developing neuromuscular synapses. Proceedings of the National Academy of Sciences. 2012; 109(39):15924–15929. doi: 10.1073/pnas.1207767109.

Johnston D, Frick A, Poolos NP. Dendrites and disease. In: *Dendrites* Oxford University Press; 2016.p. 677–702. doi: 10.1093/acprof:oso/9780198745273.003.0024.

Kepecs A, Fishell G. Interneuron cell types: fit to form and formed to fit. Nature. 2014; 505(7483):318.

Kirchner JH, Gjorgjieva J. Emergence of local and global synaptic organization on cortical dendrites. Nature Communications. 2021; 12(1):1–18.

Kirchner JH, Gjorgjieva J. Emergence of synaptic organization and computation in dendrite. Neuroforum. 2022; 28(1):21–30.

Kleindienst T, Winnubst J, Roth-Alpermann C, Bonhoeffer T, Lohmann C. Activity-dependent clustering of functional synaptic inputs on developing hippocampal dendrites. Neuron. 2011; 72(6):1012–1024.

526 **Kliemann W**. A stochastic dynamical model for the characterization of the geometrical structure of dendritic
527 processes. Bulletin of Mathematical Biology. 1987; 49(2):135–152. doi: 10.1007/BF02459695.

528 **Koene RA**, Tijms B, Van Hees P, Postma F, De Ridder A, Ramakers GJA, Van Pelt J, Van Ooyen A. NETMORPH: A
529 framework for the stochastic generation of large scale neuronal networks with realistic neuron morphologies.
530 Neuroinformatics. 2009 sep; 7(3):195–210. doi: 10.1007/s12021-009-9052-3.

531 **Koleske AJ**. Molecular mechanisms of dendrite stability. Nature Reviews Neuroscience. 2013; 14(8):536–550.

532 **Koshimizu H**, Kiyosue K, Hara T, Hazama S, Suzuki S, Uegaki K, Nagappan G, Zaitsev E, Hirokawa T, Tatsu Y,
533 et al. Multiple functions of precursor BDNF to CNS neurons: negative regulation of neurite growth, spine
534 formation and cell survival. Molecular brain. 2009; 2(1):1–19.

535 **Kroon T**, van Hugte E, van Linge L, Mansvelder HD, Meredith RM. Early postnatal development of pyramidal
536 neurons across layers of the mouse medial prefrontal cortex. Scientific reports. 2019; 9(1):1–16.

537 **Larkman A**, Mason A. Correlations Between Morphology and Electrophysiology of Pyramidal Neurons in Slices
538 of Rat Visual Cortex. I. Establishment of Cell Classes; 1990.

539 **Leighton AH**, Lohmann C. The wiring of developing sensory circuits—from patterned spontaneous activity to
540 synaptic plasticity mechanisms. Frontiers in neural circuits. 2016; 10:71.

541 **Lohmann C**, Myhr KL, Wong ROL. Transmitter-evoked local calcium release stabilizes developing dendrites.
542 Nature. 2002 jul; 418(6894):177–181. doi: 10.1038/nature00850.

543 **Lu B**, Pang PT, Woo NH. The Yin and Yang of neurotrophin action. Nature Reviews Neuroscience. 2005; 6(8):603–
544 614.

545 **Luczak A**. Spatial embedding of neuronal trees modeled by diffusive growth. Journal of Neuroscience Methods.
546 2006 oct; 157(1):132–141. doi: 10.1016/j.jneumeth.2006.03.024.

547 **Marques-Smith A**, Lyngholm D, Kaufmann AK, Stacey JA, Hoerder-Suabedissen A, Becker EBE, Wilson MC, Mol-
548 nár Z, Butt SJB. A Transient Translaminar GABAergic Interneuron Circuit Connects Thalamocortical Recipient
549 Layers in Neonatal Somatosensory Cortex. Neuron. 2016; 89(3):536–549.

550 **McAllister AK**, Lo DC, Katz LC. Neurotrophins regulate dendritic growth in developing visual cortex. Neuron.
551 1995; 15(4):791–803.

552 **Motta A**, Berning M, Boergens KM, Staffler B, Beining M, Loomba S, Hennig P, Wissler H, Helmstaedter M. Dense
553 connectomic reconstruction in layer 4 of the somatosensory cortex. Science. 2019; 366(6469):eaay3134.

554 **Naskar S**, Narducci R, Balzani E, Cwetsch AW, Tucci V, Cancedda L. The development of synaptic transmission
555 is time-locked to early social behaviors in rats. Nature Communications. 2019; 10(1):1–12.

556 **Nicholson C**, Chen KC, Hrabětová S, Tao L. Diffusion of molecules in brain extracellular space: theory and
557 experiment. Progress in brain research. 2000; 125:129–154.

558 **Niculescu D**, Michaelsen-Preusse K, Güner Ü, van Dorland R, Wierenga CJ, Lohmann C. A BDNF-Mediated
559 Push-Pull Plasticity Mechanism for Synaptic Clustering. Cell reports. 2018; 24(8):2063–2074.

560 **Niell CM**, Meyer MP, Smith SJ. In vivo imaging of synapse formation on a growing dendritic arbor. Nature
561 Neuroscience. 2004 mar; 7(3):254–260. doi: 10.1038/nn1191.

562 **Nithianandam V**, Chien CT. Actin blobs prefigure dendrite branching sites. Journal of Cell Biology. 2018;
563 217(10):3731–3746.

564 **Ohki K**, Chung S, Ch'ng YH, Kara P, Reid RC. Functional imaging with cellular resolution reveals precise micro-
565 architecture in visual cortex. Nature. 2005; 433(7026):597–603.

566 **Ooyen AV**, Van Pelt J, Corner MA. Implications of activity dependent neurite outgrowth for neuronal morphol-
567 ogy and network development. Journal of Theoretical Biology. 1995; 172(1):63–82.

568 **Park J**, Papoutsi A, Ash RT, Marin MA, Poirazi P, Smirnakis SM. Contribution of apical and basal dendrites to
569 orientation encoding in mouse V1 L2/3 pyramidal neurons. Nature Communications. 2019 dec; 10(1):1–11.
570 doi: 10.1038/s41467-019-13029-0.

571 **Payeur A**, Béïque JC, Naud R. Classes of dendritic information processing. Current opinion in neurobiology.
572 2019; 58:78–85.

573 **Poirazi P**, Brannon T, Mel BW. Pyramidal neuron as two-layer neural network. Neuron. 2003 mar; 37(6):989–
574 999. doi: 10.1016/S0896-6273(03)00149-1.

575 **Poirazi P**, Mel BW. Impact of active dendrites and structural plasticity on the memory capacity of neural tissue.
576 Neuron. 2001; 29(3):779–796. doi: 10.1016/S0896-6273(01)00252-5.

577 **Poirazi P**, Papoutsi A. Illuminating dendritic function with computational models. Nature Reviews Neuro-
578 science. 2020; 21(6):303–321.

579 **Polleux F**, Ghosh A, Grueber WB. Molecular determinants of dendrite and spine development. In: *Dendrites*
580 Oxford University Press; 2016.p. 95–128. doi: 10.1093/acprof:oso/9780198745273.003.0004.

581 **Puram SV**, Bonni A. Cell-intrinsic drivers of dendrite morphogenesis. Development. 2013; 140(23):4657–4671.

582 **Riccomagno MM**, Kolodkin AL. Sculpting Neural Circuits by Axon and Dendrite Pruning. Annual Review of Cell
583 and Developmental Biology. 2015 nov; 31(1):779–805. doi: 10.1146/annurev-cellbio-100913-013038.

584 **Richards SEV**, Moore AR, Nam AY, Saxena S, Paradis S, van Hooser SD. Experience-dependent development
585 of dendritic arbors in mouse visual cortex. Journal of Neuroscience. 2020 aug; 40(34):6536–6556. doi:
586 10.1523/JNEUROSCI.2910-19.2020.

587 **Rossi LF**, Harris K, Carandini M. Excitatory and inhibitory intracortical circuits for orientation and direction
588 selectivity. bioRxiv. 2019; p. 556795.

589 **Rudy B**, Fishell G, Lee S, Hjerling-Leffler J. Three groups of interneurons account for nearly 100% of neocortical
590 GABAergic neurons. Developmental neurobiology. 2011; 71(1):45–61.

591 **Sakai J**. How synaptic pruning shapes neural wiring during development and, possibly, in disease. Proceedings
592 of the National Academy of Sciences of the United States of America. 2020 jul; 117(28):16096–16099. doi:
593 10.1073/pnas.2010281117.

594 **Scala F**, Kobak D, Shan S, Bernaerts Y, Laturnus S, Cadwell CR, Hartmanis L, Froudarakis E, Castro JR, Tan ZH,
595 Papadopoulos S, Patel SS, Sandberg R, Berens P, Jiang X, Tolias AS. Layer 4 of mouse neocortex differs in cell
596 types and circuit organization between sensory areas. Nature Communications. 2019; 10(1):4174.

597 **Scala F**, Kobak D, Bernabucci M, Bernaerts Y, Cadwell CR, Castro JR, Hartmanis L, Jiang X, Laturnus S, Miranda E,
598 Mulherkar S, Tan ZH, Yao Z, Zeng H, Sandberg R, Berens P, Tolias AS. Phenotypic variation within and across
599 transcriptomic cell types in mouse motor cortex. Nature. 2021; 598:144—-150.

600 **Scholl B**, Wilson DE, Fitzpatrick D. Local order within global disorder: synaptic architecture of visual space.
601 Neuron. 2017; 96(5):1127–1138.

602 **Schubert D**, Kötter R, Zilles K, Luhmann HJ, Staiger JF. Cell type-specific circuits of cortical layer IV spiny neurons.
603 Journal of Neuroscience. 2003; 23(7):2961—-2970.

Sholl DA. Dendritic organization in the neurons of the visual and motor cortices of the cat. J Anat. 1953; 87:387–406.

Sretavan DW, Shatz CJ, Stryker MP. Modification of retinal ganglion cell axon morphology by prenatal infusion of tetrodotoxin. Nature. 1988; 336(6198):468–471. doi: 10.1038/336468a0.

Stepanyants A, Chklovskii DB. Neurogeometry and potential synaptic connectivity. Trends in neurosciences. 2005; 28(7):387–394.

Torben-Nielsen B, De Schutter E. Context-aware modeling of neuronal morphologies. Frontiers in Neuroanatomy. 2014 sep; 8(SEP):92. doi: 10.3389/fnana.2014.00092.

Tyler WJ, Pozzo-Miller LD. BDNF enhances quantal neurotransmitter release and increases the number of docked vesicles at the active zones of hippocampal excitatory synapses. Journal of Neuroscience. 2001; 21(12):4249–4258.

Tzilivaki A, Kastellakis G, Poirazi P. Challenging the point neuron dogma: FS basket cells as 2-stage nonlinear integrators. Nature Communications. 2019; 10(1):1–14.

Tzilivaki A, Kastellakis G, Schmitz D, Poirazi P. GABAergic interneurons with nonlinear dendrites: from neuronal computations to memory engrams. Neuroscience. 2021; .

Ultanir SK, Kim JE, Hall BJ, Deerinck T, Ellisman M, Ghosh A. Regulation of spine morphology and spine density by NMDA receptor signaling in vivo. Proceedings of the National Academy of Sciences. 2007; 104(49):19553–19558.

Uspensky JV. Introduction to mathematical probability. Proceedings of the National Academy of Sciences. 1937; .

Vaughn JE. Review: Fine structure of synaptogenesis in the vertebrate central nervous system. Synapse. 1989 jan; 3(3):255–285. doi: 10.1002/syn.890030312.

van Veen M, van Pelt J. A model for outgrowth of branching neurites. Journal of Theoretical Biology. 1992 nov; 159(1):1–23. doi: 10.1016/S0022-5193(05)80764-7.

Verhage M, Maia AS, Plomp JJ, Brussaard AB, Heeroma JH, Vermeer H, Toonen RF, Hammer RE, van den TK, Berg, et al. Synaptic assembly of the brain in the absence of neurotransmitter secretion. Science. 2000; 287(5454):864–869.

Winnubst J, Cheyne JE, Niculescu D, Lohmann C. Spontaneous activity drives local synaptic plasticity in vivo. Neuron. 2015; 87(2):399–410.

Yang J, Harte-Hargrove LC, Siao CJ, Marinic T, Clarke R, Ma Q, Jing D, LaFrancois JJ, Bath KG, Mark W, et al. proBDNF negatively regulates neuronal remodeling, synaptic transmission, and synaptic plasticity in hippocampus. Cell reports. 2014; 7(3):796–806.

Ye B, Zhang Y, Song W, Younger SH, Jan LY, Jan YN. Growing dendrites and axons differ in their reliance on the secretory pathway. Cell. 2007; 130(4):717–729.

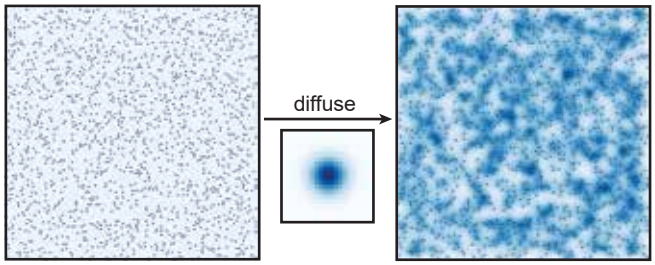

638

Figure 1–Figure supplement 1. The growth field is similar to two-dimensional heat diffusion. By iteratively convolving the potential synapses in the growth field with a Gaussian filter, the growth field reaches a steady-state that resembles a two-dimensional heat diffusion with point sources. Over time, individual point sources disappear and reappear to mimic when the corresponding synapses are connected or pruned from the dendrite.

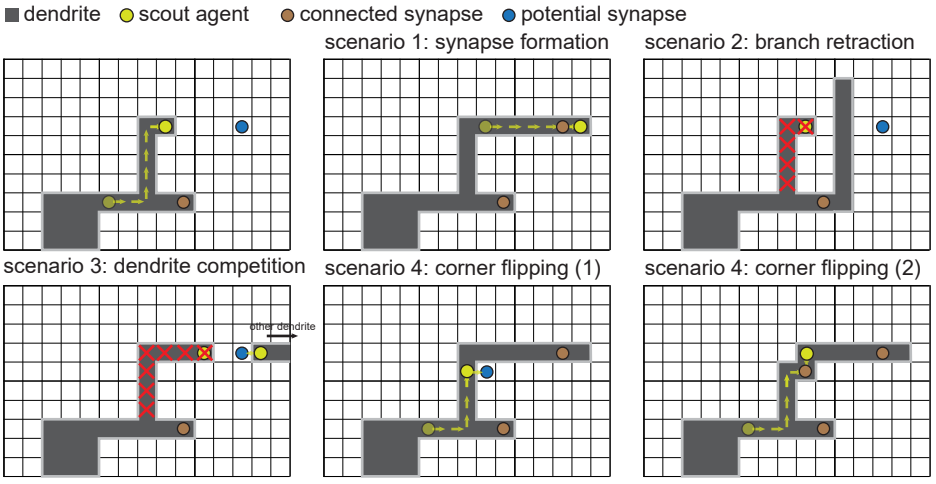

639

Figure 1–Figure supplement 2. Four scenarios of asynchronous dendritic growth can be modeled as a scout agent representing the tip of a dendrite exploring a two-dimensional grid. A scout agent (yellow dot) has reached the location of a potential synapse (blue dot). Scenario 1: The scout agent will extend the dendrite and form a new synapse if nothing else happens. Scenario 2: To prevent overlap, if a second branch from the same dendrite blocks the path to the potential synapse, the original branch retracts. Scenario 3: If a branch from another dendrite reaches the potential synapse first, the original branch retracts. Scenario 4: If a new potential synapse becomes available adjacent to the dendrite (1) so that growth is not possible (since the branch cannot form immediately adjacent to two other parts of the dendrite), the corner flips (2), and the synapse forms.

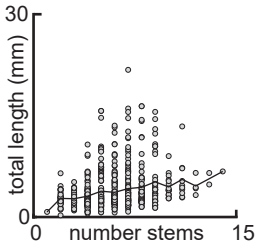

Figure 6–Figure supplement 1. Total tree length increases with the number of stems. Average (solid black) and individual (gray circles) total tree lengths as a function of the number of stems. $N = 701$. Data from the Allen Cell Types Database (2015).